American Journal of Optics and Photonics
2016; 4(4): 25-31
http://www.sciencepublishinggroup.com/j/ajop
doi: 10.11648/j.ajop.20160404.11
ISSN: 2330-8486 (Print); ISSN: 2330-8494 (Online)

The Influence of Oxygen Pressure on the Photoluminescent Properties of Pulsed Laser Ablated $SrAl_2O_4:Eu^{2+}$, Dy^{3+} Thin Films

P. D. Nsimama

Department of Science and Laboratory Technology, Dar Es Salaam Institute of Technology, Dar Es Salaam, Tanzania

Email address:
pnsimama@dit.ac.tz, nsimamapd@gmail.com, pnsimama@yahoo.com

To cite this article:
P. D. Nsimama. The Influence of Oxygen Pressure on the Photoluminescent Properties of Pulsed Laser Ablated $SrAl_2O_4:Eu^{2+}$, Dy^{3+} Thin Films. *American Journal of Optics and Photonics.* Vol. 4, No. 4, 2016, pp. 25-31. doi: 10.11648/j.ajop.20160404.11

Received: September 29, 2016; **Accepted**: October 9, 2016; **Published**: October 31, 2016

Abstract: $SrAl_2O_4:Eu^{2+}$, Dy^{3+} thin films were prepared using the pulsed laser deposition (PLD) technique and the variation of morphological, photoluminescence and structural properties with the oxygen pressure were studied. The atomic force microscopy (AFM) and scanning electron microscopy (SEM) were employed in the films morphological measurements. The He-Cd 325 nm laser photoluminescence (PL) system and xenon lamp Cary Eclipse fluorescence spectrophotometer were used to collect the photoluminescence and afterglow data. The elemental and depth profile analysis were done by using Auger electron spectroscopy (AES). $SrAl_2O_4:Eu^{2+}$, Dy^{3+} thin films gave a stable green emission peak at 523 nm, attributed to $4f^65d^1 \rightarrow 4f^7$ Eu^{2+} transitions. Superior PL and afterglow (AG) properties were recorded by the film deposited at the intermediate oxygen pressure of 0.38 Torr. The film had a rough surface as revealed by the SEM and AFM images. The AES data consisted of all the main elements in $SrAl_2O_4:Eu^{2+}$, Dy^{3+} material, i.e. Sr, Al and O and the adventitious carbon (C). The film thickness varied inversely with the oxygen pressure. The variations of Sr/Al ratios with the PL intensity are reported.

Keywords: PLD, $SrAl_2O_4:E^{u+}$, Dy^{3+}, PL, Oxygen, Sr/Al Ratio

1. Introduction

Strontium aluminate phosphors activated by Eu^{2+}, Dy^{3+} ions have attracted a lot of attention since they show excellent properties such as high quantum efficiency, long persistence of phosphorescence and good chemical stability [1]. As a result, several research groups have worked on distinguished initiatives in the course of improving its PL properties, ranging from changing the crystal phases through Sr/Al ratio variations [2], varying the concentration of rare earth dopants [3], to the use of water proof polymers, which reduce the deterioration of PL through hydrolysis [4]. Most of the published works [5–11], report on $SrAl_2O_4:E^{2+}$, Dy^{3+} phosphors prepared in powder forms. However, for various industrial applications such as device fabrication and surface coatings it is also important to investigate the performance of these phosphors in the form of thin films. However, thin film phosphors have several advantages over powders, such as higher lateral resolution from smaller grains, better thermal stability, reduced out-gassing and better adhesion to solid substrates [12].

Preparation of thin film phosphors using pulsed laser deposition (PLD) technique has become increasingly important due to several reasons including stoichiometric transfer of material from the target, generation of energetic species, hyper thermal reaction between the ablated cations and molecular oxygen in the ablation plasma, and compatibility with background pressures ranging from UHV to 100 Pa [13]. The plume kinetics depend on its interaction with the chamber atmosphere during its expansion. The chamber atmosphere strongly influences the deposition rate of ablated particles, the formation, size, and energy of the clusters during the PLD process [14].

In our previous work [15] we reported on the effects of gas atmospheres on the properties of $SrAl_2O_4:Eu^{2+}$, Dy^{3+} thin films prepared by pulsed laser deposition. We observed that films ablated in the gas atmospheres had better photoluminescence and afterglow properties compared with the film prepared in vacuum. Two gas types (oxygen and argon) were involved and their gas pressures were fixed at

0.34 Torr. However, it is of great importance to study the influence of individual gas pressures on the properties of pulsed laser ablated $SrAl_2O_4:Eu^{2+}$, Dy^{3+} films on a relatively broader range (lower to higher values) of gas pressures to identify the optimum range for better phosphor properties. Oxygen pressure has been reported [16] to mainly determine the atomic kinetic energy of an oxide material when the laser energy and substrate temperature are fixed.

The current work reports on the influence of oxygen gas pressures on the morphological, photoluminescence and structural properties of pulsed laser deposited $SrAl_2O_4:Eu^{2+}$, Dy^{3+} thin films. Three different values of oxygen pressure were introduced into the chamber and the PL properties of the deposited films were studied. The changes of maximum PL intensity, initial AG intensity and maximum Sr/Al ratio with the oxygen pressure are discussed.

2. Experimental Details

The PLD deposition chamber was evacuated to a base pressure of 8×10^{-6} mbar. The Lambda Physic 248 nm KrF excimer laser was used to ablate the phosphor pellet prepared from a commercial $SrAl_2O_4:Eu^{2+}$, Dy^{3+} phosphor from a UK phosphor company in the oxygen atmospheres. The oxygen (purity 99.999 %) pressure was varied during depositions while keeping other deposition parameters constant, in which the substrate temperature, substrate-distance, laser fluence and the number of pulses were fixed at 600℃, 6 cm, 1.27 J/cm^2 and 25000 respectively. The films were deposited on 1 cm^2 Si (111) substrates.

The AFM images were obtained from the Shimadzu SPM - 9600 model. The SIEMMENS D5000 diffractometer using CuKα radiation of λ = 1.5405 nm was employed for XRD data collection. The PL data were collected in air at room temperature using a He-Cd 325 nm laser as an excitation source. The afterglow measurements were done by using a Cary Eclipse fluorescence spectrophotometer (Model: LS 55) with a built-in xenon lamp and a grating to select a suitable wavelength for excitation. The excitation wavelength was 340 nm and the slit width was 20 nm. The PHI 700 Auger Nanoprobe was used to take SEM images and monitor the surface composition during electron bombardment. The thin films were bombarded with a primary electron beam (25 kV, 10 nA) for AES survey analyses at a pressure of 1 x 10^{-9} Torr. The depth profiles analyses were done with a kV 2 μA 2x2 raster Ar ion beam, 1x1 mm raster area and sputter rate of 27 nm per min.

3. Results and Discussion

3.1. SEM Results

Figure 1 shows the SEM images for $SrAl_2O_4:Eu^{2+}$, Dy^{3+} thin films deposited at different oxygen pressures. The surface of the film deposited at the lowest oxygen pressure of 0.19 Torr has its surface covered with varying sizes of spherical and conical shaped phosphor particulates. They look like molten parts of the target, exploded during ablation. The film's surface of the sample deposited at the intermediate (0.38 Torr) oxygen pressure has only few small irregular shaped particulates. Cracks are also observed on its surface possibly resulting from a mismatch between the silicon substrate and the deposited film. The increase in surface roughness with increasing O_2 pressure may be attributed to an enhanced particulate formation in the laser induced flume, which is a typical characteristic of high-pressure laser ablation [17]. However, at higher oxygen pressures the roughness decreases due to the reduction of plume speed which necessitates a slower nucleation growth to take place at the substrate. The surface seems to be the roughest of all. The film deposited at high (0.81 Torr) oxygen pressure has a uniform surface with very few spherical particulates of varying sizes.

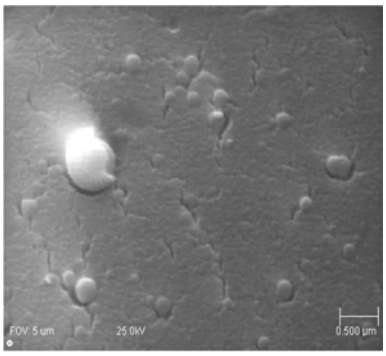

(a)

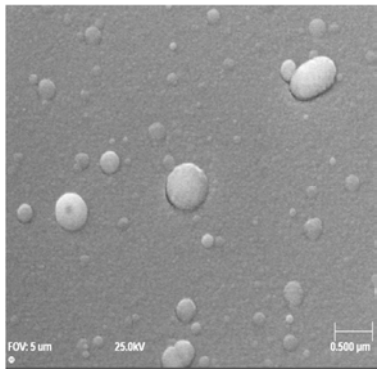

(b)

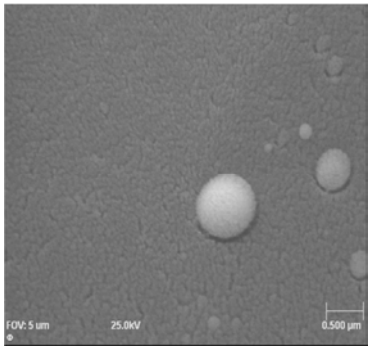

(c)

Figure 1. *The SEM images for $SrAl_2O_4:E^{u+},Dy^{3+}$ thin films deposited at different oxygen pressures (a) 0.19 Torr (b) 0.38 Torr and (c) 0.81 Torr.*

3.2. AFM Results

The AFM images of $SrAl_2O_4:Eu^{2+},Dy^{3+}$ thin films ablated at different oxygen pressures are shown in Figures 2. The film deposited at 0.19 Torr oxygen pressure has poorly defined grains, which is possibly due to the fact that at low oxygen pressure, collisions between atoms in plasma plume and oxygen atoms could be very weak; hence the surface adatoms have high kinetic energy. High energy can create defects in the growing film [18] leading to poorly defined grains. The agglomeration is observed on this film forming heaps of grain particles. The AFM image of the film prepared at intermediate (0.38 Torr) oxygen pressure has well defined grains. On the other hand, morphology of the AFM image of the film deposited at highest oxygen pressure (0.81 Torr) is similar to that deposited at intermediate (0.38 Torr) oxygen pressure. The only noted difference is the allignment of nanoparticles in which the film deposited at 0.38 Torr are vertically oriented while those deposited at 0.81 Torr are slanted towards one side.

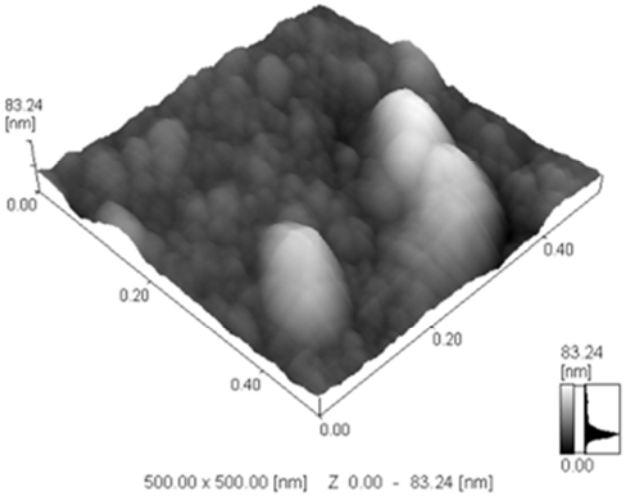

(a)

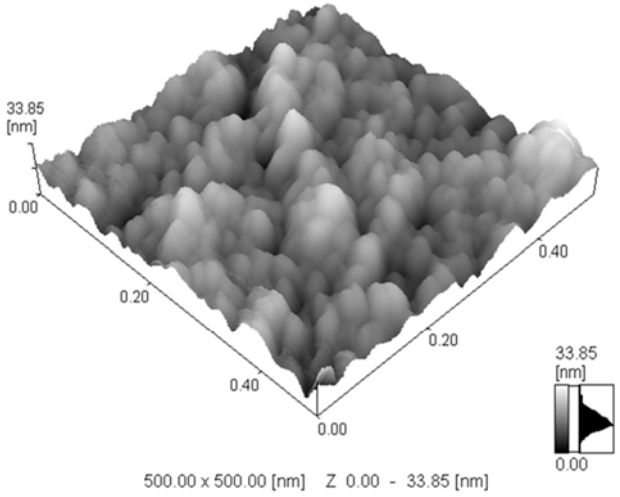

(b)

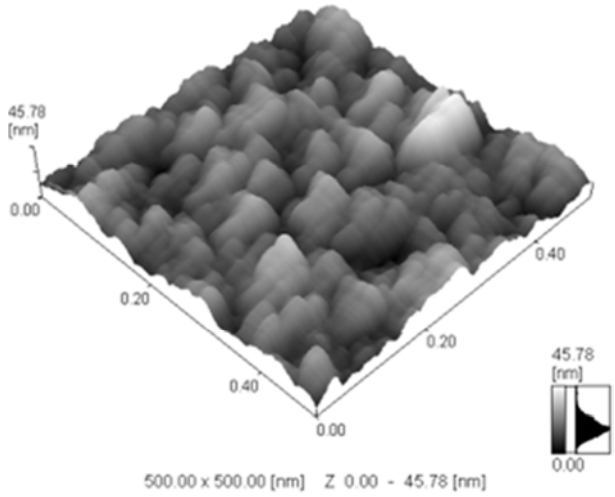

(c)

Figure 2. *The AFM images of $SrAl_2O_4:E^{u+},Dy^{3+}$ thin films ablated at different oxygen pressures (a) 0.19 Torr (b) 0.38 Torr and (c) 0.81 Torr.*

3.3. XRD Results

The XRD results for our as-deposited thin films were all amorphous (not shown). Amorphous structures for the as-deposited $SrAl_2O_4:Eu^{2+}$, Dy^{3+} thin films have also been reported from our previous works [12, 15].

3.4. Photoluminescence (PL) Results

The room temperature PL results for the $SrAl_2O_4:Eu^{2+}$, Dy^{3+} films deposited at different oxygen pressures are shown in Figure 3. All the films have one prominent green emission peak at 523 nm attributed to the $4f^65d^1 \rightarrow 4f^7$ Eu^{2+} transitions. The highest peak is recorded by the film that was deposited at the intermediate (0.38 Torr) oxygen pressure followed by the film deposited at low (0.19 Torr) oxygen pressure. The lowest PL intensity was coming from the film deposited at highest (0.81 Torr) oxygen pressure.

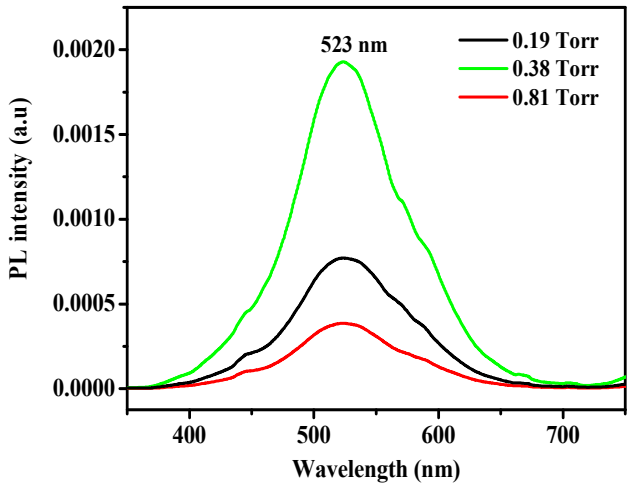

Figure 3. *The room temperature photoluminescence spectra for $SrAl_2O_4:Eu^{2+}$, Dy^{3+} thin films deposited at different oxygen pressures.*

Figure 4 shows the long afterglow (phosphorescence)

characteristics of $SrAl_2O_4:Eu^{2+},Dy^{3+}$ thin films deposited at different oxygen pressures. Consistent with the PL data in Figure 3, the film prepared at oxygen pressure of 0.38 Torr has the highest initial afterglow intensity followed by the film deposited at the oxygen pressure of 0.19 Torr and lastly is the one deposited at 0.81 Torr.

Since all the films had amorphous XRD structures, we attribute the difference in their PL and afterglow properties to the differences in morphological and the depth profiles of the films. The thicknesses of the films (from the depth profile analysis; section 3.5) were 459 nm, 445.5 nm and 283.5 nm for the films deposited at 0.19 Torr, 0.38 Torr and 0.81 Torr respectively. It is therefore reasonable to argue that the best PL and afterglow properties of the $SrAl_2O_4:E^{u+},Dy^{3+}$ thin film deposited at 0.38 Torr is attributed to the large thickness, surface roughness and well defined grains of the film as revealed by the AFM images. This follows from the previous works [12, 15], where it was reported that $SrAl_2O_4:Eu^{2+},Dy^{3+}$ thin films with well defined AFM grains, large thickness and rough films gave superior PL and afterglow properties. The other two films have relatively inferior PL properties because they don't posses both properties. The poorest PL and afterglow properties were from the film prepared at the oxygen pressure of 0.81 Torr.

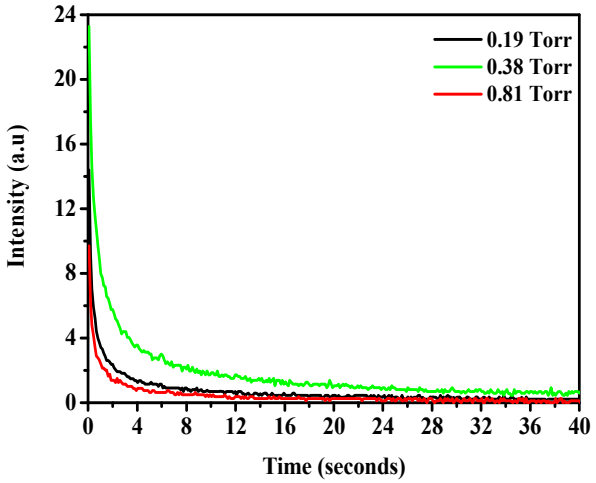

Figure 4. *The afterglow curves for PLD $SrAl_2O_4:Eu^{2+},Dy^{3+}$, Dy3+ thin films deposited at different oxygen pressures.*

3.5. Auger Electron Spectroscopy Results

Figure 5 shows the AES depth profile analyses in atomic concentration for the $SrAl_2O_4:Eu^{2+},Dy^{3+}$ thin films prepared at oxygen pressures 0.19 Torr (Figure 5 (a)), 0.38 Torr (Figure 5 (b)) and 0.81 Torr (Figure 5 (c)). The depth profiles from the three films are having all the main elements in the $SrAl_2O_4:Eu^{2+}$, Dy^{3+} material, i.e. Sr, Al, and O. The other two elements displayed in the figures are not part of the sample; these are the C and Si from the atmospheric contamination the substrate respectively. The dopants Eu^{2+} and Dy^{3+} could not be identified, possibly because of their small quantities in the $SrAl_2O_4:Eu^{2+}$, Dy^{3+} material. In all the samples, the magnitudes of atomic concentrations take a decreasing order from O to Sr to Al. The films show good uniformity of elemental atomic concentrations for the entire range. A sharp decrease in the atomic concentrations of C in the first five minutes is observed in all figures substantiating that C was on the top layer and was likely coming from contaminations.

In Figure 5 (b), the Sr atomic concentration is almost the same as that of O and an overlapping is observed between the two. This is different from the case of Figure 5 (a), where the atomic percentage of O is higher than that of Sr almost throughout the entire film thickness. This is possibly due to the scattering effect from the background oxygen molecules. It seems the traveling of Sr atoms across the oxygen molecules was easier than O, because Sr is heavier (87.62 g) than oxygen (15.999 g). The scattering from O could not deflect it away from the direction normal to the target. Generally, during the expansion in a background gas there is a preferential propagation of the heavy atoms along the normal (which usually is the direction of the substrate) [19].

The sputtering rate for all the films was 27 nm/min. Based on the film sputtering time to reach the Si substrate (Si atomic concentration ≥ 95 %) the thicknesses for the films deposited at 0.19 Torr, 0.38 Torr and 0.81 Torr were approximately 351 nm, 324 nm and 81 nm respectively.

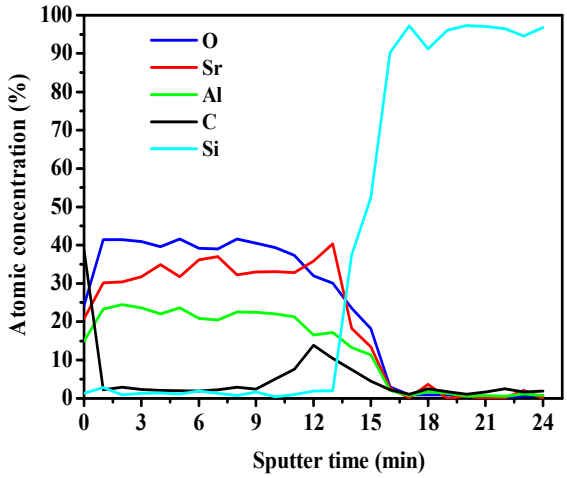

(a)

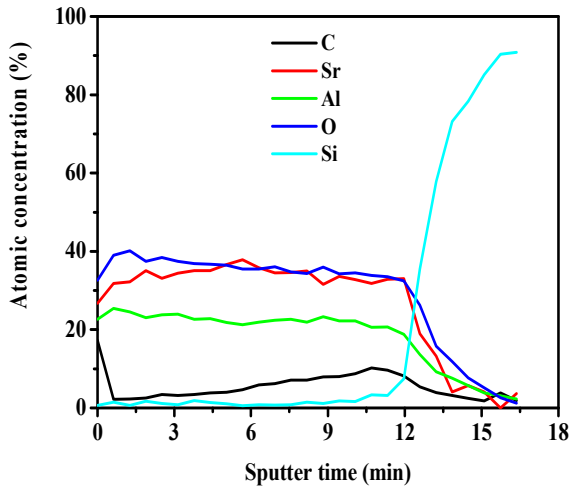

(b)

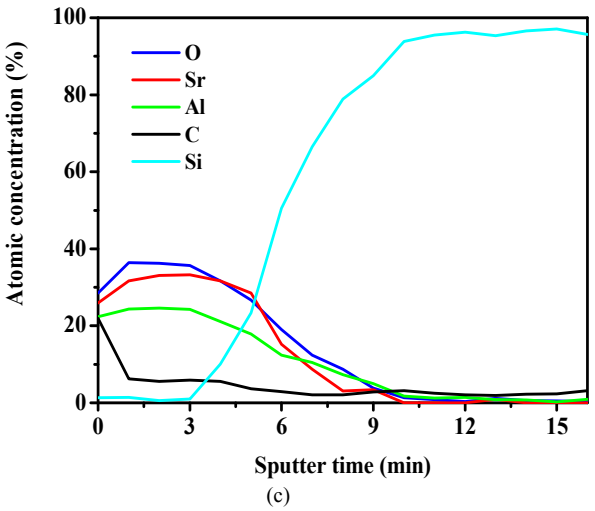

(c)

Figure 5. *The AES depth profile spectra of $SrAl_2O_4:Eu^{2+}$, Dy^{3+} thin films deposited at oxygen pressure (a) 0.19 Torr (b) 0.38 Torr and (c) 0.81 Torr.*

The decrease in film thickness at higher oxygen pressure is due to the fact that the kinetic energy of atoms in plasma plume is decreased by collision with the ambient gas resulting in the thinnest film for a sample which is deposited at highest oxygen pressure [16]. Similar results were reported elsewhere [20] whereby the deposition rate of indium phosphide (InP) was decreasing with the increase of the argon pressure. Obtaining thicker films initially and thinner ones with the increase in oxygen pressure is in agreement with findings on other materials reported elsewhere [21]. They noted that as one increases the background gas pressure there will first be an increase in deposition rate, especially for species such as Ba, Sr, Pb and Ag which show large re-sputtering yields, due to quenching of the energetic species and subsequent reduction in re-sputtering. This will then be followed by a decrease in deposition rate due to the plume being strongly scattered by the gas and becoming less.

The AES elemental surveys for SAED thin films before and after depth profiles were similar and Figure 6 is showing the survey for the highest emitting film, i.e., the sample deposited at 0.38 Torr.

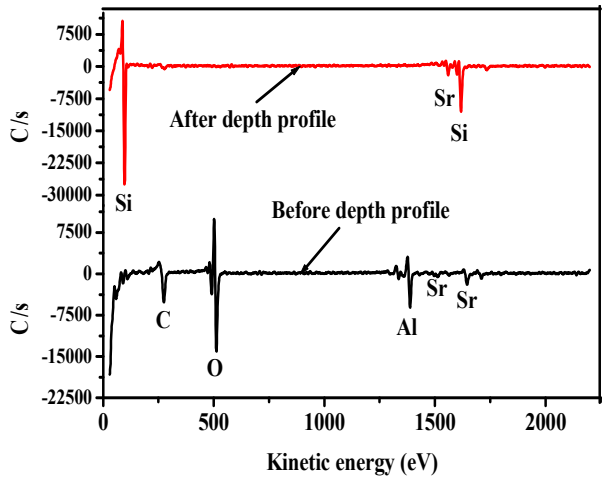

Figure 6. *The AES elemental analysis for the optimum $SrAl_2O_4:Eu^{2+}$, Dy^{3+} thin film before and after depth profile.*

The AES survey before the depth profile shows the presence of all main elements of $SrAl_2O_4:Eu^{2+}$, Dy^{3+} material plus the adventitious carbon. The AES survey after the depth profile is mainly having Si, (substrate) signifying that the film layer was almost all sputtered out.

The comparisons of elemental atomic concentrations across the film are given by Figure 7 (a)-7(c) for the oxygen (O), strontium (Sr) and Aluminium (Al) respectively. The O atomic concentration was highest (Figure 7 (a)) in the film deposited at 0.19 Torr and decreased with the increase in oxygen pressure in the background. It seems that at low oxygen pressure, oxygen atoms from the target could be easily transported through the plume and deposited on the substrate. As the background oxygen pressure was increased the atomic concentration decreased due to the deflection of the plume particles by the increased number of oxygen molecules.

The comparisons of Sr atomic concentrations for the three films (Figure 7 (b)) indicate a slightly non-uniform trend for films deposited at 0.19 and 0.38 Torr. The Sr atomic concentration for the film deposited at 0.38 Torr was generally higher than that of O. This is possibly due to the scattering by the background oxygen molecules of the O atoms. The scattering could not significantly affect Sr because is heavier (87.62 g) than oxygen (15.999 g).

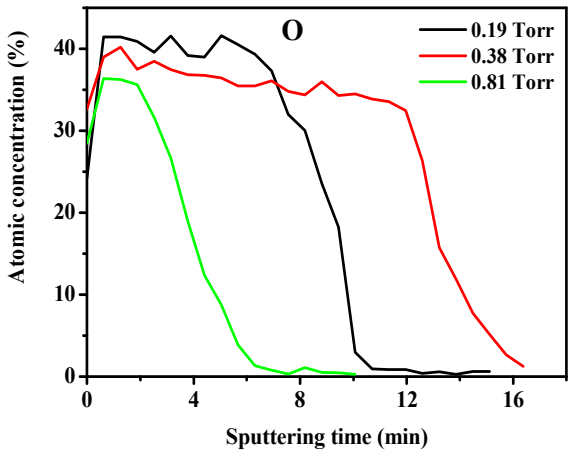

(a)

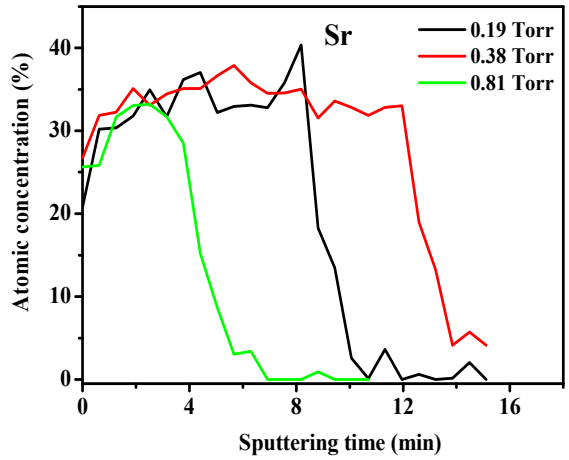

(b)

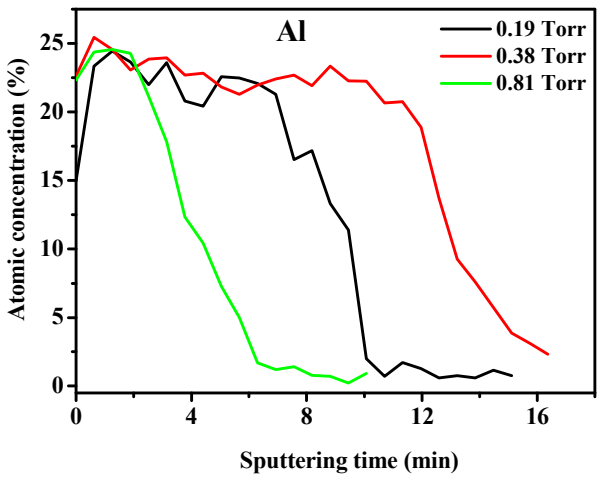

(c)

Figure 7. *Depth profile elemental atomic concentration (a) O (b) Sr and (c) Al across the films deposited at 0.19 Torr, 0.38 Torr and 0.81 Torr oxygen pressures.*

Figure 7 (c) shows the Al atomic concentration across the films deposited at different oxygen pressures. The highest emitting film recorded the highest concentration followed by the film deposited at 0.81 Torr. The Al concentration surpassed that of the film deposited at 0.19 Torr possibly due to it being heavier (26.892 g) than the background gas (O). Generally, the elemental atomic concentrations for the film deposited at 0.38 Torr were of good uniformity for the entire film layer.

The variation of maximum PL intensity and maximum afterglow initial intensity with Sr/Al ratio for the films prepared at different oxygen pressures is shown in Figure 8. The Sr/Al ratio seems to be the main determining factor for the PL and afterglow properties of SAED thin films as the three vary proportionally. The highest PL and initial afterglow intensities were recorded by the sample deposited at the oxygen pressure of 0.38 Torr. The variation of elemental atomic composition for this sample (Figure 7) showed almost uniform distribution across the film.

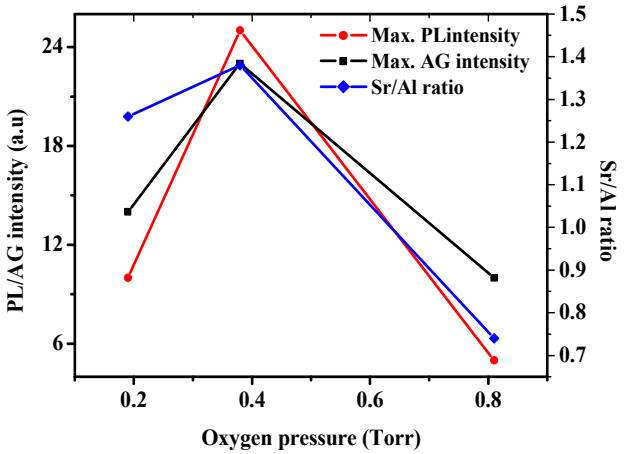

Figure 8. *Variation of maximum PL intensity and initial afterglow (AG) intensity with the Sr/Al ratio for SAED deposited at oxygen pressure 0.19 Torr, 0.38 Torr and 0.81 Torr.*

It is reasonable to conclude from this result that the best PL and afterglow properties for the films are recorded by the sample deposited at the maximum Sr/Al ratio.

4. Conclusion

$SrAl_2O_4:Eu^{2+},Dy^{3+}$ thin film phosphors were successfully ablated on Si substrate by pulsed laser deposition technique. The photoluminescence properties of $SrAl_2O_4:Eu^{2+}$, Dy^{3+} thin films change with the oxygen pressure. The film deposited at the intermediate oxygen pressure (0.38 Torr) gave the highest PL and afterglow properties of the $SrAl_2O_4:Eu^{2+}$, Dy^{3+} thin films. The film had a rough surface as revealed by the AFM and SEM images. Only one prominent PL peak was observed at wavelength 523 nm attributed to the $4f^65d^1 \rightarrow 4f^7$ transitions of Eu^{2+} ions. The depth profile results show a lower film thickness at high background oxygen pressure. The AES survey analysis shows that the films contains all the main elements, Sr, O and Al of $SrAl_2O_4:Eu^{2+}$, Dy^{3+}. The oxygen pressure seems to control the Sr/Al ratio of the ablated films. The maximum PL and AG properties of the $SrAl_2O_4:Eu^{2+}$, Dy^{3+} thin films was recorded by the film that has the maximum Sr/Al ratio.

Acknowledgements

The African Laser Centre (ALC), National Research Fund (NRF) and the Nano materials cluster program of the University of the Free State are highly acknowledged for their financial support.

References

[1] S. D Han, K. C. Singh, T. Y. Cho, H. S. Lee, D. Jakhar, J. P. Hulme, C. H. Han, J. D. Kim, II-S. Chun, J. Gwak, (2008), J. Lumin. 128, 301–305.

[2] Wen-Zhou Sun, Yu-Hong Chen, Lan-Er Wu and Yong Jiang, (2013), Rare Metals, 32, 414-419.

[3] A. Kumar, G. Kedawat, P. Kumar, J. Dwivedi and B. K Gupta, (2015), New Journal of Chemistry, 39, 3380-3387.

[4] M. P Anesh, S. Gulrez, A. Anis, S. al-Zahrani, (2014), Advances in Polymer Technology, DOI:10.1002/adv.21436.

[5] Huayna Terraschke, Markus Suta, Matthias Adlung, Samira Mammadova, Nahida Musayeva, Rasim Jabbarov, Mihil Nararov and Claudia Wickleder, Journal of Spectroscopy, Volume 2015, Article ID 541958, 12 pages.

[6] Y. L Chang, H. I Hsiang, M. T Sai Liang, (2008), J. Alloys Compds. 461, 598–603.

[7] P. D Sarkisov, N. V. Popovich, A. G. Zhelnin, (2003), Glass Ceram. 60, 9–10.

[8] T. Peng, L. Huajun, H. Yang, (2004), J. Mater. Chem. Phys. 85, 68–72.

[9] T. Peng, H.Yang, X. Pu, B. Hu, Z. Jian, C. Yan, (2004), Mater. Lett. 58, 352–356.

[10] X. Li, Y. Qu, X. Xie, Z. Wang, R. Li, (2006), Mater. Lett. 60, 3673–3677.

[11] Vishal Sharma, Amrita Das, Vinay Kumar, (2016), Mater. Res. Expr. 3, 01504.

[12] P. D Nsimama, M. O. Ntwaeaborwa, E. Coetsee, H. C. Swart, (2009), Physica B; Condensed Matter, 404, 4489-4492.

[13] A. M. Hristea, O. Alm, E. Jeane, P. Boman, (2004), Thin Solid Films 516, 8431-8435.

[14] A. Bailini, P. M. Ossi, A. Rivolta, (2007), Appl. Surf. Sci. 253, 7682–7685.

[15] P. D Nsimama, M. O. Ntwaeaborwa, H. C. Swart, (2011), Journal of Lum. 131, 119-125.

[16] Z. G Zhang, F. Zhou, X. Q. Wei, M. Liu, G. Sun, C. S. Chen, C. S. Xue, H. Z. Zhuang, B. Y. Man, (2007), Physica E 39, 253-257.

[17] S. S. Kim, B. T. Lee, (2004), Thin Solid Films 446, 307-312.

[18] D. P Norton, (2004), Mater. Sci. Eng. R 43 139–247.

[19] J. Schou, (2009), Appl. Surf. Sci. 255, 5191-5198.

[20] M. A. Hafez, K. A. Elamrawi, H. E. Elsayed-Ali, (2004), Appl. Surf. Sci. 233, 42-50.

[21] P. R Willmott, (2004), Prog. Surf. Sci. 76, 163-217.